MR Imaging Findings in Spinal Ligamentous Injury

Philip F. Benedetti[1], Linda M. Fahr[2], Lawrence R. Kuhns[3], L. Anne Hayman[2,4,5]

Clinical instability of the spine after trauma occurs when the spinal ligaments and bones lose their ability to maintain normal alignment between vertebral segments while they are under a physiologic load. Instability can lead to further injury, pain, or deformity and can require surgical stabilization. MR imaging has been shown to be helpful in the detection of ligamentous injury [1]. The purpose of this study is to familiarize the reader with the MR imaging appearance of these injuries. This article is divided into three sections. The first illustrates injuries to the complex craniocervical junction. The second reviews the remainder of the spine, and the third addresses the technical factors that optimize the detection of spinal ligamentous injury.

The importance of these MR findings is increasing as clinicians begin to compare outcomes and treatments for specific types of ligamentous injury detected on MR imaging

Fig. 1.—Normal anatomy in 21-year-old man. Sagittal T1-weighted MR image (TR/TE, 510/25) obtained on 0.3-T scanner shows normal apical ligament (1) and anterior atlantoaxial membrane (2).

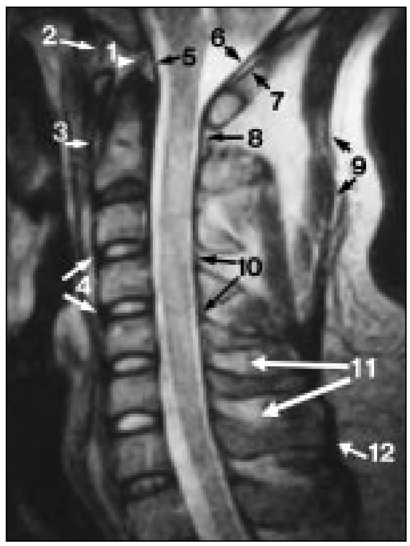

Fig. 2.—Normal anatomy in 43-year-old woman. Sagittal T2-weighted MR image (TR/TE, 4500/117) obtained on 0.3-T MR scanner shows normal apical ligament (1), anterior occipitoatlantal membrane (2), anterior atlantoaxial membrane (3), anterior longitudinal ligament (4), tectorial membrane (5), dural reflection (6), posterior occipitoatlantal membrane (7), posterior atlantoaxial membrane (8), nuchal ligament (9), flaval ligaments (10), area of interspinous ligaments (11), and supraspinous ligament (12).

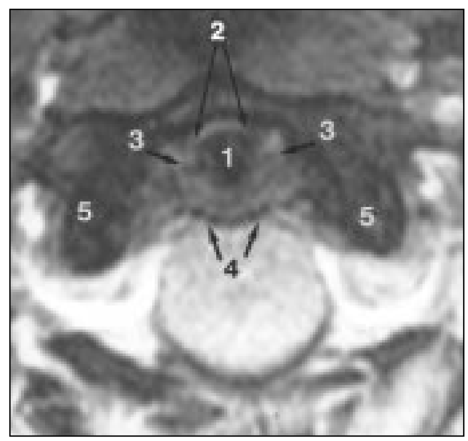

Fig. 3.—Normal anatomy in 38-year-old man. Axial gradient-echo or fast low-angle shot MR image (TR/TE, 420/18; flip angle, 30°) obtained on 1.0-T MR scanner shows dens (1), presumed anterior atlantodental ligaments (2), alar ligaments (3), transverse ligament (4), and lateral masses of C1 (5).

Received November 11, 1999; accepted after revision February 2, 2000.

Presented at the annual meeting of the American Roentgen Ray Society, New Orleans, May 1999.

[1] Medford Radiological Group, 692 Murphy Rd., Medford, OR 97504.

[2] Department of Radiology, Baylor College of Medicine, One Baylor Plaza, Houston, TX 77030. Address correspondence to L. A. Hayman.

[3] Department of Pediatric Radiology, F3503, University of Michigan, 1500 E. Medical Center Dr., Ann Arbor, MI 48109.

[4] Department of Psychiatry and Behavioral Sciences, Baylor College of Medicine, Houston, TX 77030.

[5] Herbert J. Frensley Center for Imaging Research, Baylor College of Medicine, Houston, TX 77030.

AJR 2000;175:661–665 0361–803X/00/1753–661 © American Roentgen Ray Society

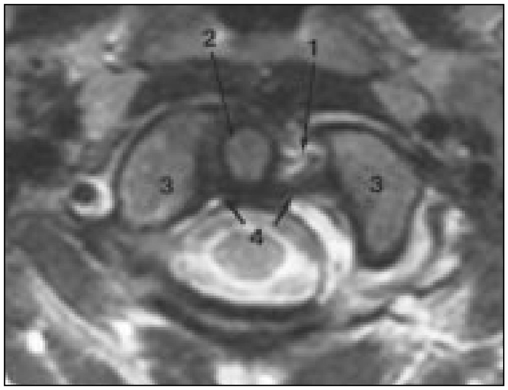

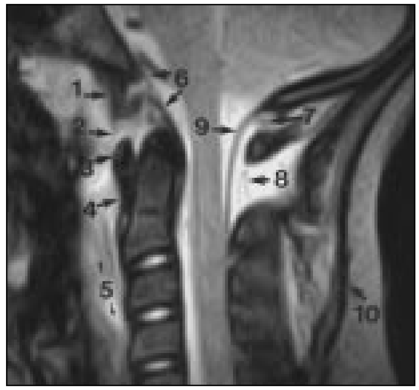

A

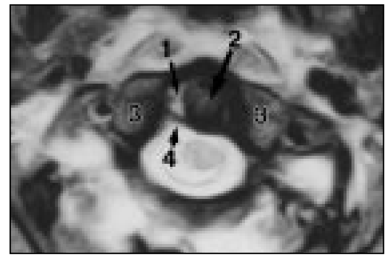

B

Fig. 4.—Left alar ligament tear in 19-year-old woman with severe neck pain after fall on her head while snowboarding. Fixed deviation of dens to right was seen on radiograph (not shown). C1–2 rotatory subluxation was suspected. Axial T2-weighted MR image (TR/TE, 4000/90) obtained on 1.0-T MR scanner shows isolated tear of left alar ligament (1) and deviation of dens (2) toward right with respect to lateral masses of C2 (3). Transverse ligament (4) is intact. Sagittal images (not shown) depict normal alignment of occipital condyles with C2, thus no rotatory subluxation is present. CT performed before MR imaging was negative for fracture and fixed rotatory subluxation. These results allowed confident symptomatic treatment that led to full recovery.

Fig. 5.—Occipitoatlantal dislocation in 11-year-old boy who was neurologically intact after motor vehicle crash.
A, Sagittal gradient-echo MR image (TR/TE, 510/35; flip angle, 20°) obtained on 0.3-T MR scanner shows intact (1) and torn (2) portions of anterior occipitoatlantal membrane, anterior arch of C1 (3), intact anterior atlantoaxial membrane (4), prevertebral edema or hemorrhage (5), torn tectorial membrane (6), torn posterior occipitoatlantal membrane (7), torn posterior atlantoaxial membrane (8), intact dural reflection (9), and intact nuchal ligament (10). Before MR imaging, full extent of injury and degree of instability were not appreciated either clinically or from results of radiographs or CT scans. Patient underwent surgical fusion shortly thereafter.
B, Axial gradient-echo MR image (510/35; flip angle, 20°) obtained on 0.3-T MR scanner shows torn right alar ligament (1), displacement of dens (2) to left with respect to lateral masses of C2 (3), and intact transverse ligament (4).

[2–8]. As this information grows, so does the power of MR imaging to guide treatment and to enable prediction of outcome.

Craniocervical Injuries

Many ligaments are seen normally at the craniocervical junction (Fig. 1). However, only three are considered the major stabilizers. These are the tectorial membrane (Fig. 2), the transverse ligament, and the alar ligaments (Fig. 3). The normal tectorial membrane and transverse ligament are routinely seen on MR imaging, whereas the normal alar ligaments can be more difficult to visualize because of lack of contrast from adjacent tissues (Fig. 3). In most individuals, each alar ligament arises from the lateral margin of the dens, then courses laterally in a near-vertical plane, attaching to both the ipsilateral occipital condyle and the subjacent superior margin of the lateral mass of the atlas (C1). However, in about a third of individuals, these ligaments insert solely onto the occiput. The alar ligaments limit axial rotation at the occipitoatlantoaxial complex. Blood or edema adjacent to an acute alar ligament tear (Figs. 4 and 5) improves visualization of these ligaments. Secondary evidence of ligamentous injury to one of the alar ligaments is displacement of the dens to the contralateral side. Isolated posttraumatic alar ligament tears have been classified. These are clinically significant because hypermobility at the atlantoaxial joint can reduce blood flow in the contralateral vertebral artery. Hulse [9] describes "cervical nystagmus as a manifestation of vertebral artery insufficiency due to rotatory hypermobility at the occipitoatlanto-axial complex." Figure 6 shows displaced ligament injuries at the craniocervical junction associated with a type II dens fracture.

Cervical, Thoracic, and Lumbar Injuries

Figures 7 and 8 show ligamentous injury associated with a burst fracture of the cervical vertebrae. Figures 9–11 picture injuries caused by cervical hyperextension. Injuries associated with interfacetal dislocations and teardrop fractures are also shown in Figures 12–14.

The concept of three columns of support in the thoracic and lumbar spine is well ac-

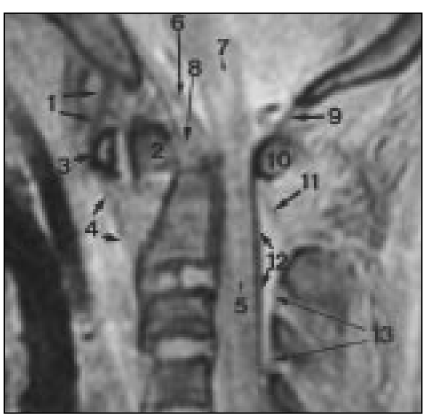

A

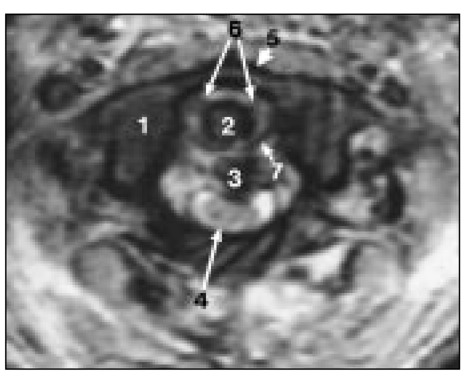

B

Fig. 6.—Type II dens fracture in 14-year-old boy who was unrestrained passenger in motor vehicle crash.
A, Sagittal gradient-echo MR image (TR/TE, 500/9; flip angle, 15°) obtained on 1.5-T MR scanner shows intact occipitoatlantal membrane (1), anterior dislocation of fractured dens (2), anterior arch of C1 (3), partial tear of anterior atlantoaxial membrane (4), cord contusion (5), intact dura (6), medullary contusion or edema (7), torn tectorial membrane (8), intact posterior occipitoatlantal membrane (9), posterior arch of C1 (10), torn or attenuated posterior atlantoaxial membrane (11), intact dura (12), and intact flaval ligaments (13).
B, Axial gradient-echo MR image (250/15; flip angle, 15°) obtained on 1.5-T MR scanner shows right lateral mass of C1 (1), anteriorly dislocated dens (2), body of C2 at fracture site (3), compressed and contused spinal cord (4), anterior arch of C1 (5), intact alar ligaments (6), and intact transverse ligament (7).

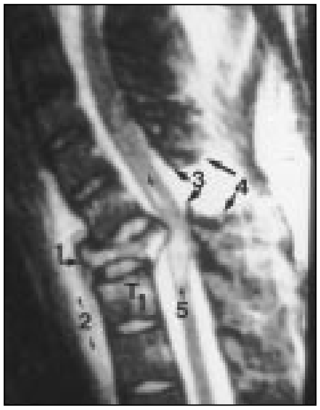

Fig. 7.—Burst fracture of C7 in 30-year-old woman who was unrestrained driver in motor vehicle crash. Sagittal fast spin-echo inversion-recovery MR image (TR/TE, 3000/51; inversion time,140 msec) obtained on 1.5-T MR scanner shows burst fracture of C7 (1), prevertebral edema or hemorrhage (2), flaval (3) and interspinous ligament tears (4), with associated distraction of dorsal spines and spinal cord contusion (5). Also note signal hyperintensity caused by bone marrow edema in vertebral bodies of C6 and T1.

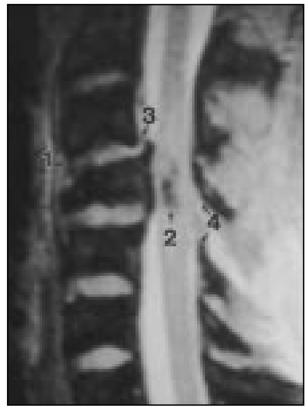

Fig. 8.—Burst fracture of C4 with retropulsion in 17-year-old boy after motor vehicle crash. Sagittal gradient-echo MR image (TR/TE, 650/13; flip angle, 15°) obtained on 1.5-T MR scanner shows anterior longitudinal ligament tear (1), hypointense hemorrhagic cord contusion (2), posterior longitudinal ligament tear at C3–4 (3), and flaval ligament tear at C4–5 (4).

cepted. The same principles have been applied to the C3–C7 vertebral levels in the cervical spine. Stability is provided by intact osseous and ligamentous structures. The anterior column consists of the anterior vertebral body, the anterior longitudinal ligament, and the anterior annulus fibrosus. The middle column comprises the posterior vertebral body, the posterior longitudinal ligament, and the posterior annulus fibrosus. Hyperextension can result in injury to the anterior column (Fig. 10) or to both the anterior and middle columns (Figs. 11 and 15). The posterior column consists of the posterior elements of the spine, ligamentum flavum, interspinous ligaments, supraspinous ligaments, and facet joint capsules. Hyperflexion may result in injury to the middle and posterior columns (Figs. 9 and 16). Injury to any two adjacent columns will result in instability. Disruption of all three osseous or ligamentous supporting columns is shown in association with burst fractures in Figures 7 and 8, bilateral interfacetal dislocation is shown in Figures 12 and 13, and teardrop fractures of C7 are shown in Figure 14.

Imaging Considerations

Successful MR imaging of spinal trauma depends on several factors. One of these is the timing of the study. Although no research has yet, to our knowledge, defined the optimal time interval between injury and MR imaging, it should probably be less than 72 hr [8]. Beyond this time, resorption of the edema or hemorrhage reduces sensitivity of MR imaging to reveal injuries. Specifically, the T2 signal hyperintensity produced by edema or extravasation of blood into injured extradural tissues provides an excellent contrast medium, improving the conspicuity of the ligaments that are usually of low signal intensity on all imaging sequences.

The use of appropriate sequence parameters for MR imaging is also important. These parameters vary widely according to the field

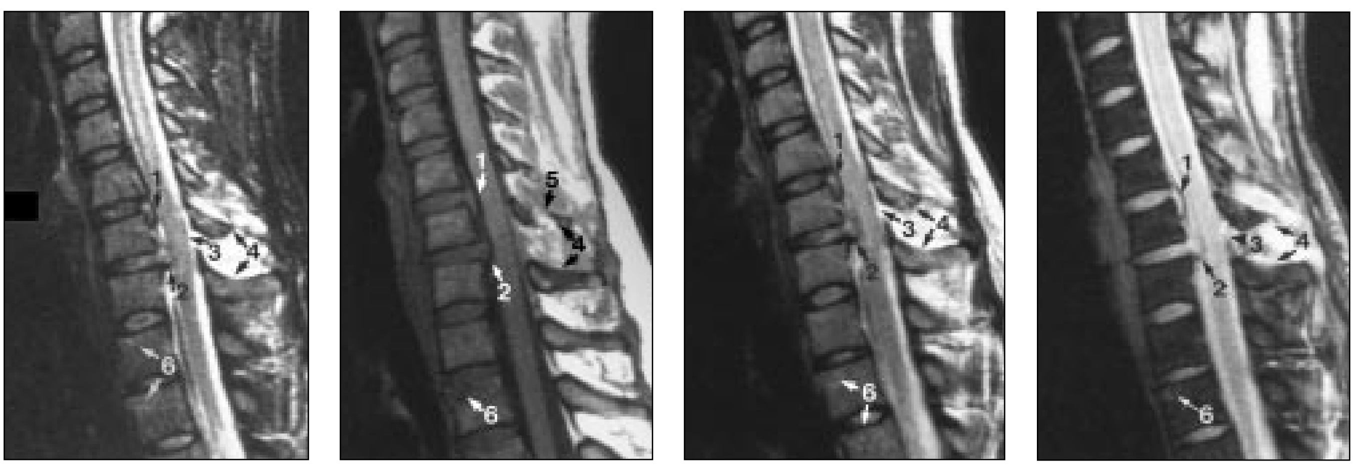

A B C D

Fig. 9.—35-year old woman involved in head-on motor vehicle collision who presented with severe neck pain, right arm pain, and numbness. Radiographs and CT scans (not shown) showed negative findings. Four pulse sequences from a 1.0-T MR scanner at midsagittal level are provided to allow reader to compare and contrast abnormalities. Findings include disk extrusion and inferior stripping of posterior longitudinal ligament at C5–6 (1); disk extrusion and tear of posterior longitudinal ligament and annulus fibrosus at C6–7 (2); flaval ligament tear at C6–7 (3); splaying of dorsal spines and interspinous ligament tear at C6–7 (4); fracture of C6 spinous process (5); and mild superior endplate impaction fractures of T1, T2, and T3 vertebral bodies (6). Solely on basis of results of MR images, the following day patient was started in traction and taken to surgery where anterior diskectomy and fusion at C5–6 and C6–7 were performed. Patient experienced immediate marked improvement in symptoms after surgery.

A, Fast spin-echo inversion-recovery sagittal MR image (TR/TE, 4000/60; inversion time, 140 msec) best shows bone marrow edema caused by fracture or trabecular contusion, spinal cord injury, and soft-tissue edema.

B, T1-weighted MR image (500/15) is helpful in showing anatomic detail and alignment and in detecting fracture.

C, T2-weighted fast spin-echo MR images (3500/90), like this one, are often best for showing ligaments, blood in spinal cord, bone marrow edema, and soft-tissue edema.

D, Gradient-echo MR images (500/18; flip angle, 30°), like this one, are often best for showing ligaments and blood in spinal cord.

strength, coil design, gradient strength, and software capabilities of the MR imaging system used. Thus, each system requires an individualized approach, fine-tuned by trial and error. In general, field of view, slice thickness, matrix, and signal averages must be chosen to balance the effects on signal-to-noise ratio, spatial resolution, and imaging times. For example, longer imaging times may improve scan quality but provide more opportunity for patient motion. A typical MR imaging protocol for spinal trauma should include the following sequences in the sagittal plane: T1-weighted, fast spin-echo T2-weighted, gradient-echo, and fast spin-echo inversion-recovery images. In the axial plane, protocol should include gradient-echo or T2-weighted images. Optional coronal T1-weighted or gradient-echo sequences can aid in evaluation of the cranioatlantoaxial segment, especially with regard to alignment and dens fracture. Figure 9 compares the relative merits of the four sagittal sequences described previously. T1-weighted images provide the best ana-

10

11

Fig. 10.—Hyperextension injury in 71-year-old man who fell from bicycle and presented with central cord syndrome. Sagittal T2-weighted MR image (TR/TE, 4500/117) obtained on 0.3-T MR scanner shows flaval ligament hypertrophy (1), C5–6 posterior disk protrusion (2), anterior longitudinal ligament tear, and partial disruption of C5–6 intervertebral disk (3).

Fig. 11.—6-year-old boy with cervical spine hyperextension injury during motor vehicle crash. Sagittal fast spin-echo inversion-recovery MR image (TR/TE, 3000/51; inversion time, 140 msec) obtained on 1.5-T MR scanner shows horizontal fracture through inferior endplate of C6 (1), posterior longitudinal ligament tear (2), cord contusion (3), anterior longitudinal ligament tear (4), prevertebral hemorrhage or edema (5), and extradural hemorrhage (6). MR imaging findings guided therapy resulting in anterior surgical fusion.

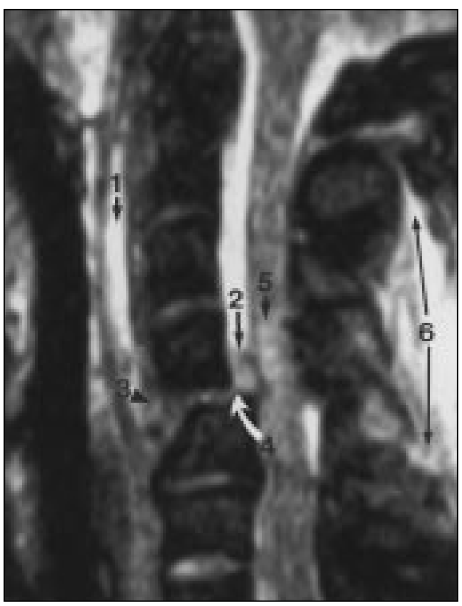

Fig. 12.—Bilateral interfacetal dislocation at C4–5 in 62-year-old man involved in motor vehicle crash. Sagittal gradient-echo MR image (TR/TE, 510/35; flip angle, 20°) obtained on 0.3-T MR scanner shows prevertebral edema or hemorrhage (1), posterior longitudinal ligament tear (2), anterior longitudinal ligament tear (3), large traumatic posterior disk extrusion (4), cord contusion and compression (5), posterior paravertebral edema or hemorrhage, and probable interspinous ligament injury (6).

Fig. 13.—Bilateral interfacetal dislocation in 42-year-old woman involved in motor vehicle crash. Sagittal T2-weighted MR image (TR/TE, 4500/117) obtained on 0.3-T MR scanner shows tear of dura and posterior atlantoaxial membrane (1), partial tear of nuchal ligament (2), distraction of C5–6 spinous process and torn interspinous ligaments (3), torn flaval ligaments (4), torn posterior longitudinal ligament (5), and torn anterior longitudinal ligament (6).

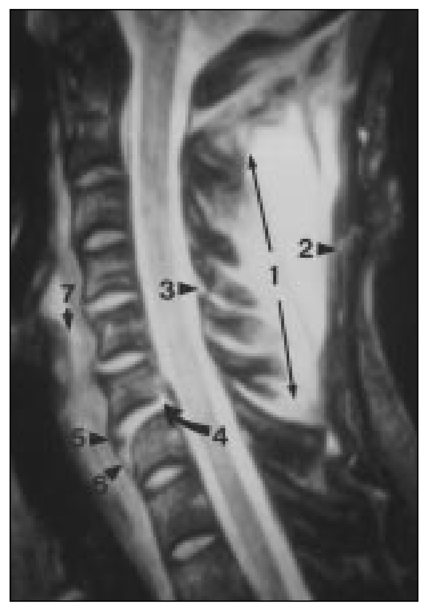

Fig. 14.—Teardrop fracture of C7 in 27-year-old man involved in motor vehicle crash. Sagittal gradient-echo MR image (TR/TE, 510/35; flip angle, 20°) obtained on 0.3-T MR scanner shows extensive posterior paravertebral edema or hemorrhage and probable tearing of interspinous ligaments (1), partial tear of nuchal ligament (2), flaval ligament tear (3), partial tear of posterior longitudinal ligament (4), anterior superior corner fracture of C7 vertebral body (5), stripping of anterior longitudinal ligament from anterior surface of C7 vertebral body (6), and prevertebral edema or hemorrhage (7).

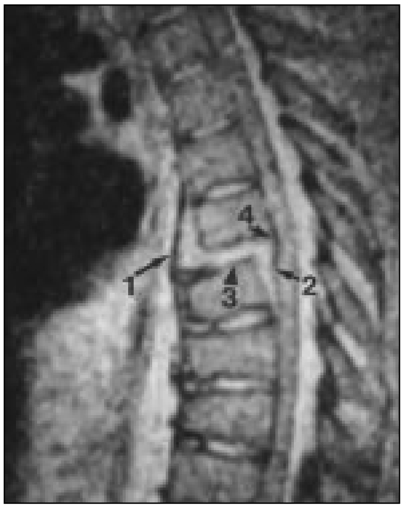

Fig. 15.—Ligament stripping in 450-lb (202.5-kg) 35-year-old man ejected from motor vehicle. Lateral radiographs (not shown) were nondiagnostic. Sagittal gradient-echo MR image (TR/TE, 510/35; flip angle, 20°) obtained on 0.3-T MR scanner shows anterior longitudinal ligament stripped completely away from anterior surface of midthoracic spine vertebral body (1). Similarly, posterior longitudinal ligament is stripped away from posterior vertebral body surface at level of fracture-subluxation (2). Adjacent intervertebral disk is disrupted (3) and thoracic spinal cord is compressed (4).

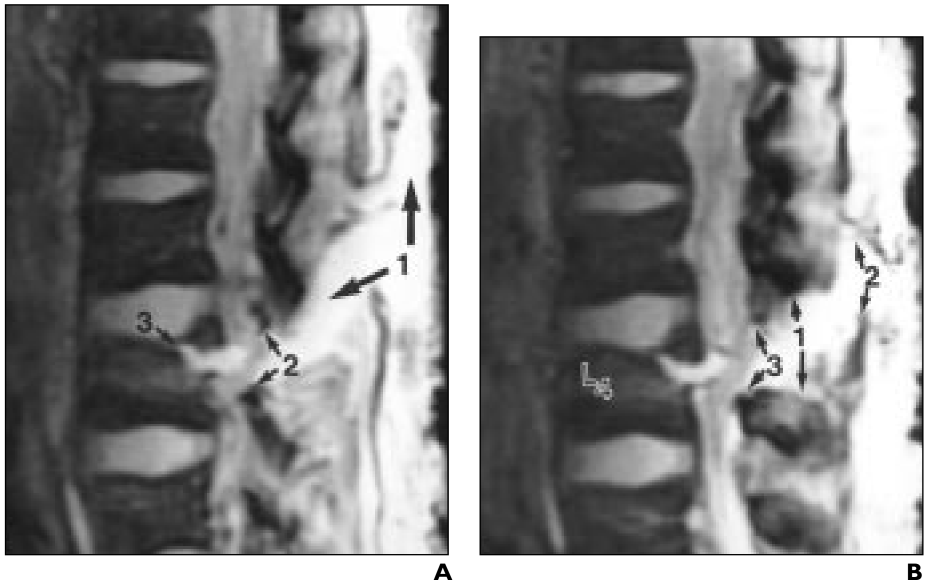

Fig. 16.—11-year-old boy who suffered flexion–distraction injury from lap belt during motor vehicle crash with fractures at L4 level.
A, Sagittal gradient-echo MR image (TR/TE, 500/13; flip angle, 15°) obtained on 1.5-T MR scanner shows large presumed cerebrospinal fluid leak into posterior subcutaneous tissues (1), distracted fracture fragments of left L4 articular processes (similar fracture was also present on right) (2), and distracted fracture, near horizontal in orientation, involving posterosuperior portion of L4 vertebral body (3).
B, Sagittal gradient-echo MR image (500/13; flip angle, 15°) obtained on 1.5-T MR scanner of midline shows distraction of spinous process of L3 and L4 (1), supraspinous ligament tear (2), and flaval ligament tear (3).

tomic detail, accurately depict alignment, and are invaluable for detection of fracture. Ligaments are usually best seen on gradient-echo and T2-weighted sequences. At high field strength, the heterogeneity effect produced by gradient-echo imaging techniques results in greater sensitivity for detection of blood products within the spinal cord but also reduces signal intensity within bone and makes fracture detection more difficult. At low field strength, the gradient-echo heterogeneity effect is weaker so that blood products are less easily detected but fracture detection is somewhat improved. T2-weighted and fast spin-echo inversion-recovery sequences are most sensitive for bone marrow edema (caused by fracture or trabecular contusion), spinal cord injury, and soft-tissue edema. Cerebrospinal fluid pulsatility artifacts and truncation artifacts can sometimes interfere with spinal cord evaluation on T2-weighted and fast spin-echo inversion-recovery sequences.

Conclusion

MR imaging of the posttraumatic spine is a rapidly evolving technique with the potential to revolutionize the evaluation and treatment of ligamentous injuries. In our clinical experience, it has been an invaluable adjunctive technique, particularly in patients with relevant neurologic deficits and those requiring closed reduction of a posttraumatic spinal subluxation. It has also been helpful in evaluating spinal trauma complicated by altered sensorium, extreme obesity, or even malingering.

References

1. Katzberg RW, Benedetti PF, Drake CM, et al. Acute cervical spine injuries: prospective MR imaging assessment at a level 1 trauma center. *Radiology* **1999**;213:203–211
2. Keiper ZRA, Bilaneui LT. MRI assessment of the supportive soft tissues of the cervical spine in acute trauma in children. *Neuroradiology* **1998**;40:359–363
3. Halliday AL, Henderson BR, Hart BL, Benzel EC. The management of unilateral lateral mass/facet fractures of the subaxial cervical spine. *Spine* **1997**;22:2614–2621
4. Davis SJ, Teresi LM, Bradley WG, Siemba MA, Bloze AE. Cervical spine hyperextension injuries: MR findings. *Radiology* **1991**;180:245–251
5. Brightman RP, Miller CA, Rea GL, Chakeres DW, Hunt WE. Magnetic resonance imaging of trauma to the thoracic and lumbar spine: the importance of the posterior longitudinal ligament. *Spine* **1992**;17:541–550
6. Saifuddin A, Noordeen H, Taylor BA, Bayley I. The role of imaging in the diagnosis and management of thoracolumbar burst fractures: current concepts and a review of the literature. *Skeletal Radiol* **1996**;25:603–613
7. Petersilge CS, Pathria MN, Emery SE, Masaryk TJ. Thoracolumbar burst fractures: evaluation with MR imaging. *Radiology* **1995**;194:49–54
8. Selden NR, Quint DJ, Patel N, d'Arcy HS, Papadopoulos SM. Emergency magnetic resonance imaging of cervical spinal cord injuries: clinical correlation and prognosis. *Neurosurgery* **1999**;44:785–792
9. Hulse M. Differential diagnosis of vertigo in functional cervical vertebrae joint syndromes and vertebrobasilar insufficiency [in German]. *HNO* **1982**;30:440–446